



6-4-5

DYNAMIC PROPERTIES OF R.C. COLUMNS WITH DIFFERENT REINFORCEMENT RATIOS UNDER LATERAL LOADINGS

Koichi TAMURA¹ and Sigeaki MORICHI¹

¹Department of Civil Engineering, Science University of Tokyo
Noda-shi, Chiba-ken, Japan

SUMMARY

The purpose of the experiment is to study static and dynamic behaviors of reinforced concrete columns in the plastic range. As static tests, lateral alternating loads were applied at the top slab and increased or decreased in steps. After each static test, forced vibration test was performed by steps. Linear vibration equations for the specimen were analysed, with damping ratio and stiffness obtained by experiments and it was found that the calculated resonant frequency and amplitude were almost the same as the values of experiment, though behaviour of the specimens showed nonlinear condition.

INTRODUCTION

Reinforced concrete columns are apt to receive serious damages in strong earthquakes even now. Also, linear and nonlinear behaviours of R C columns have been studied by many researchers and they proposed several equations representing the relation between load and deformation. However, in design of R C structures, dynamic response analyses for earthquakes have been performed in the range of elastic properties, except some special cases. Therefore, it is thought useful to study the limit of linear analysis for the behaviour of R C columns.

EXPERIMENT

Specimens Column specimens with longitudinal reinforcement of 6-D10, 12-D10 and 10-D13 were chosen as the subject. Dimensions were 10x20 cm in cross-section and 102.5 cm in height. (Fig. 1) They were fixed at the base and tied to a top slab by embedding longitudinal bars with quality of SD-30. The desired concrete strength was 300 kgf/cm² but the average cylinder strength of No. 1, No. 2 and No. 3 specimen were 281 kgf/cm² at age 10 days, 196 kgf/cm² at 7 days and 183 kgf/cm² at 7 days. Their assumed strength f'_c at 28 days were 406, 336 and 311 kgf/cm² respectively.

Static Test The situation of the test is

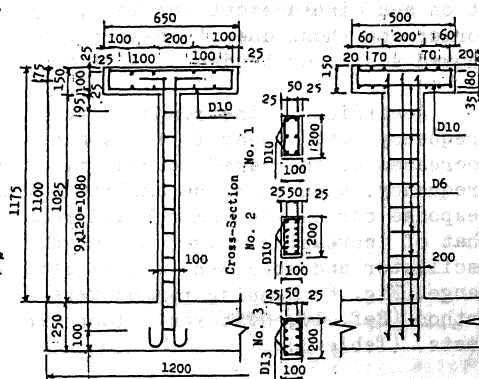


Fig. 1 Column Specimen

shown in Fig. 2. A lateral load was increased in one direction up to the appointed load and reduced, and then increased in the opposite direction in the same way. Load, displacement of the slab and rotation at the base of the column were measured. Load displacement curves due to flexural deformation and base rotation were similar and showed ellipses in general but inverted S type near

Table 1 Static Test Results

No.	Load (kg)	Total Dis (mm)	D F (mm)	D R (mm)	$\frac{HK_v}{3EI}$
1-1	100	3.08	2.31	0.77	3.00000
2	200	6.61	4.83	1.78	2.71348
3	300	12.68	9.45	3.23	2.92570
4	400	19.08	14.00	5.08	2.75591
5	500	47.07	22.08	24.99	0.88355
6	600	85.44	36.62	48.82	0.75010
2-1	200	3.26	2.69	0.57	4.71930
2	400	8.76	7.10	1.66	4.27711
3	600	15.07	11.77	3.30	3.56515
4	800	22.05	16.92	5.13	3.29825
5	1000	29.85	22.99	6.86	3.35131
6	1057	57.25	35.11	22.14	1.58559
3-1	400	7.02	5.54	1.48	3.75593
2	800	17.64	12.97	4.67	2.78028
3	1200	30.68	21.66	9.02	2.40133
4	1490	49.69	28.37	21.32	1.33068

D F, D R: Displacement due to Flexural Deformation or Rotation at the Base

Table 2 Forced Vibration Test

No.	mr (kg cm)	R I		R D	
		Freq (Hz)	Amp. (mm)	Freq (Hz)	Amp. (mm)
1-1	5	4.53	5.55	4.20	3.15
2	5	4.35	7.00	4.08	4.95
3	9	3.79	10.75	3.53	7.20
4	13	3.58	20.1	3.13	10.25
5	50	2.54	31.55	2.31	22.45
6	50	2.25	28.85	2.16	22.05
2-1	3	6.11	4.45	5.83	2.75
2	7	5.31	10.6	5.10	6.95
3	10	4.88	18.35	4.57	9.40
4	13	4.71	25.65	4.42	13.85
5	20	4.53	31.55	4.08	15.65
6	50	3.76	30.2	3.57	24.90
3-1	7	5.64	10.65	5.54	10.05
2	15	5.21	20.3	4.95	11.25
3	35	4.64	32.85	4.20	16.20
4	50	3.95	41.15	3.59	24.90

mr: Eccentric Mass Moment
R I, R D: Resonant Response in Increasing or Decreasing Exciting Frequency

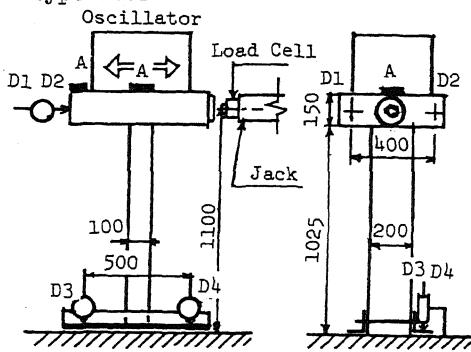


Fig. 2 Test Apparatus

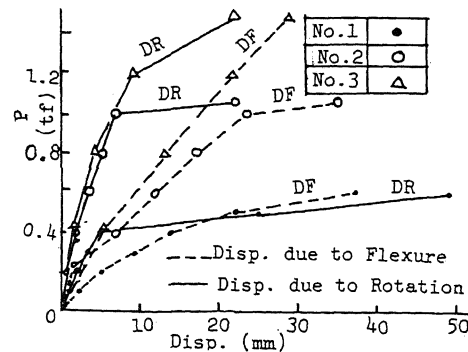


Fig. 3 Load and Displacement at the Slab

failure with many horizontal cracks. (Fig. 3 and 4)

Forced Vibration Test The oscillator was EX50DC made by Ito-Seiki Co. with maximum exciting force and frequency of 1 tf and 30 Hz. Its eccentric mass moment was adjusted, so that maximum amplitude occurred close to static displacement but did not exceed it at each stage. At the test, exciting frequency was increased from zero to 7 Hz and then reduced from 7 Hz to zero. Utilizing the record of acceleration and displacement obtained, response amplitude-frequency curves from the former and those due to base rotation from the latter were drawn. These showed a similar tendency, indicating vibration forms of the first mode.

According to the response curves in increasing frequency stage, amplitude and frequency were linear till resonance. However, response amplitude and frequency decreased or increased several times as a sawtooth in spite of increasing exciting frequency, when response amplitude was lowering. In case of decreasing frequency, response curves were smooth and resonant frequency and amplitude were smaller than that of increasing stage, as shown in Table 2 and Fig. 5. Phase difference between oscillator and specimen was smooth, same as an usual test, except the unstable range. (Fig. 6) Damping ratios were obtained from response curves by Half-power Method (Ref. 1), hysteresis loops in static tests (Ref. 2) and free vibration tests. (Table 3)

ANALYSIS

Free Vibration Assuming that a column has elastic uniform property and a slab and an oscillator are rigid body, free vibration equations are as follows. (Fig. 7)

$$\frac{\partial^2 Y}{\partial t^2} + v^2 \frac{\partial^4 Y}{\partial x^4} = 0, \quad v^2 = \frac{EIg}{wA} \quad (1)$$

where, w: weight per unit length of a column

A: cross-section of a column

EI: flexural rigidity of a column

g: acceleration of gravity

Solution of eq. (1) is given by assuming

$$y = X(x) \cdot e^{int}, \quad \lambda^4 = n^2/v^2$$

$$X = C_1 \cos \lambda x + C_2 \sin \lambda x + C_3 \cosh \lambda x + C_4 \sinh \lambda x \quad (2)$$

Coefficients are determined from boundary conditions. When it is defined that I_0 and W_0 are weight moment of inertia and weight of the sum of an oscillator and a slab, and K_r is rotation spring constant, the ratio of displacement at the slab height H due to flexural deformation to that due to rotation at the base is expressed as follows.

$$\frac{HK_r}{3EI} = \frac{\lambda H \sin \lambda h \cosh \lambda h (1 + 2W_0 a \lambda^2 / wA - W_0 \lambda^4 I_0 / (wA^2)) + \cos \lambda h \sinh \lambda h (-1 + 2W_0 \lambda^2 a / wA - 3 \sin \lambda h \cosh \lambda h (I_0 \lambda^3 + W_0 \lambda + W_0 \lambda^3 a^2) / wA + \cos \lambda h \sinh \lambda h (W_0 \lambda - I_0 \lambda^3 + W_0 \lambda^4 I_0 / (wA^2)) + 2 \cos \lambda h \cdot \cosh \lambda h (I_0 \lambda^3 / wA + W_0 \lambda^2 a^2 / wA) + 2W_0 \lambda \sin \lambda h \sinh \lambda h / wA}{-W_0 \lambda^3 a^2 / wA + \cos \lambda h \cosh \lambda h (1 - W_0 \lambda^4 I_0 / (wA^2)) - 2W_0 \lambda^2 a \sin \lambda h \sinh \lambda h / wA} \quad (3)$$

Free vibration mode shape X is expressed as follows, if C_4 is assumed as unity.

$$X = K \left(\cos \lambda h + \cosh \lambda h - W_0 \lambda (\sin \lambda h - \sinh \lambda h) / wA - W_0 \lambda a (\cos \lambda h - \cosh \lambda h) / wA \right) \cos \lambda x / 2EI \lambda + (-\cosh \lambda h - W_0 \lambda \sin \lambda h / wA - W_0 \lambda a \cosh \lambda h / wA + K_r (\sin \lambda h - \sinh \lambda h + W_0 \lambda (\cos \lambda h - \cosh \lambda h) / wA - W_0 \lambda a (\sin \lambda h + \sinh \lambda h) / wA) / 2EI \lambda) \sin \lambda x + K \left(-\cos \lambda h - \cosh \lambda h + W_0 \lambda (\sin \lambda h - \sinh \lambda h) / wA + W_0 \lambda a (\cos \lambda h - \cosh \lambda h) / wA \right) \cosh \lambda x / 2EI \lambda + (-\cos \lambda h + W_0 \lambda \sin \lambda h / wA + W_0 \lambda a \cdot \cos \lambda h / wA - K_r (\sin \lambda h - \sinh \lambda h + W_0 \lambda (\sin \lambda h - \sinh \lambda h) / wA - W_0 \lambda a (\cos \lambda h - \cosh \lambda h) / wA) / 2EI \lambda) \sinh \lambda x$$

Table 3 Damping Ratio

No.	Forced Vib.	H L	Free Vib.
1-1	0.0239	0.027	
2	0.0149	0.030	
3	0.0184	0.032	
4	0.0139	0.026	
5	0.0393	0.10	
6	0.0449	0.22	
2-1	0.0156	0.029	
2	0.0122	0.027	
3	0.0103	0.019	
4	0.0106	0.015	
5	0.0132	0.020	
6	0.0440	0.18	
3-1	0.0106	0.021	0.0211
2	0.0123	0.016	0.0212
3	0.0194	0.014	0.0365
4	0.0228	0.083	0.0265

H L: Damping due to Hysteresis Loop

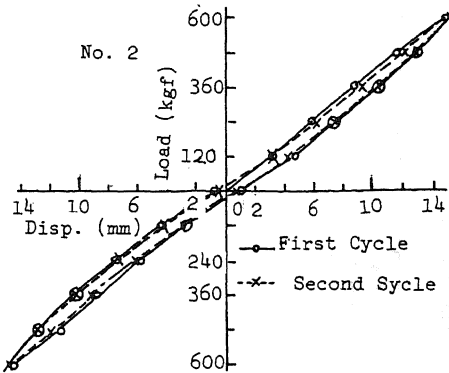


Fig. 4 Static Cycle Load and Displacement

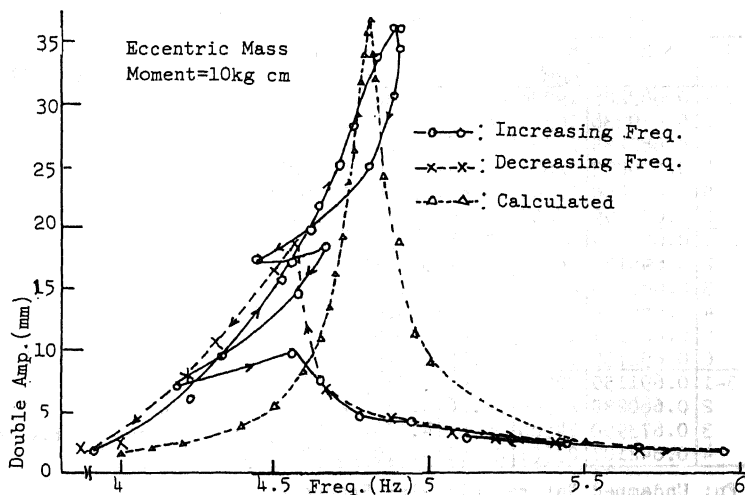


Fig. 5 Response Curve (No. 2-3)

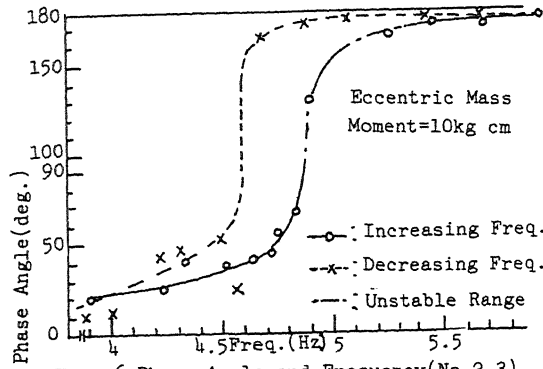


Fig. 6 Phase Angle and Frequency (No.2-3)

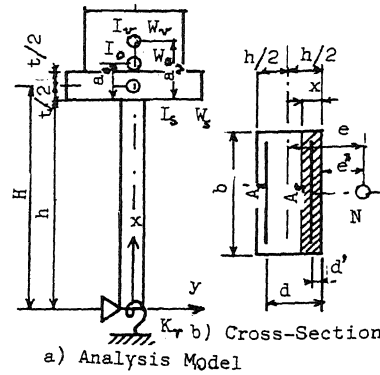


Fig. 7 Calculation Model

$$\frac{(\cos \lambda h - \cosh \lambda h) / W_v - W_v a (\sin \lambda h + \sinh \lambda h) / W_v}{2EI \lambda} \sinh \lambda x \quad (4)$$

In calculation, W_v , I_v , a , W_s and I_s are 160 kgf, 6.35 kgf m², 0.325 m, 121.9 kgf and 4.52 kgf m² respectively. As the first mode vibration, natural circular frequency and mode shape at several points were calculated, applying the static displacement ratios of flexural deformation to base rotation in Table 1. As natural frequencies of the second mode are apart from that of the first mode and the effective mass of the first mode is about 90 % of the total mass, it can be assumed that the vibration form shows mainly first mode shape and has little effects of other modes.

Forced Vibration If orthogonality relationships can be assumed (Ref. 1) in forced vibration including damping, n_m mode vibration due to exciting force $P \cos \omega t$ is as follows.

$$\ddot{q}_m + 2 h_m n_m \dot{q}_m + n_m^2 q_m = X_m P \cos \omega t \cdot M_m, \quad M_m = \sum \frac{X_m^2 W}{g} \quad (5)$$

Then, special solution under steady-state response is

$$q = X_m P \cos(\omega t - \alpha) / M_m \sqrt{(n_m^2 - \omega^2)^2 + 4 h_m^2 n_m^2 \omega^2} \quad (6)$$

$$\alpha = \tan^{-1} \frac{2 h_m n_m \omega}{n_m^2 - \omega^2}$$

Then, maximum amplitude and frequency n_r at resonance are

$$q_m = P X_m / 2 h_m n_m^2 M_m \sqrt{1 - h_m^2}, \quad n_r = n_m \sqrt{1 - 2 h_m^2} \quad (7)$$

Table 4 Results of Analysis (First Mode)

No.	$\lambda_1 h$	EI (kgm ²)	Fn (Hz)	Fr (Hz)	Mn (kg)	Amp. (mm/kg)	$\lambda_2 h$
1-1	0.683225	19206	27.26	4.336	22.7100	1.027	2.08061
2	0.679238	18371	26.35	4.193	22.7484	1.761	2.07426
3	0.682255	14085	23.28	3.704	22.7194	1.828	2.07905
4	0.679873	12676	21.93	3.490	22.7423	2.726	2.07526
5	0.613458	10047	15.86	2.526	23.3085	1.822	1.99340
6	0.600599	7269	12.96	2.058	23.4021	2.397	1.98171
2-1	0.697934	32986	37.28	5.932	22.5640	0.843	2.10590
2	0.695164	24995	32.19	5.123	22.5920	1.444	2.04966
3	0.689436	22626	30.13	4.795	22.6492	1.951	2.03992
4	0.686734	20977	28.78	4.580	22.6758	2.077	2.08637
5	0.687301	19298	27.65	4.400	22.6702	1.807	2.08732
6	0.652739	13359	20.75	3.296	22.9906	0.959	1.98709
3-1	0.691159	32034	36.03	5.733	22.6321	1.326	2.04280
2	0.680230	27366	32.26	5.133	22.7389	1.424	2.02519
3	0.673990	24580	30.01	4.775	22.7982	1.042	2.06620
4	0.642107	23301	26.52	4.219	23.0814	1.131	2.02375

Fn: Undamped Natural Circular Frequency
Fr: Resonant Frequency $\lambda_2 h$: Second Mode

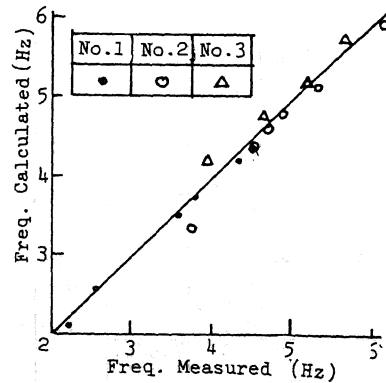


Fig. 8 Resonant Frequency Measured and Calculated

Resonant frequency and amplitude due to 1 kgf exciting force are also shown in Table 4, where damping ratio by Half-Power Method is applied. Measured and calculated resonant amplitude and frequency are drawn in Fig. 8 and 9. As an example, calculated response curve is overlapped in Fig. 5. As a result, calculated frequencies were similar to the measured values and calculated amplitudes were in approximate agreement with experiments but shapes of response curves were different from experiments.

Flexural Stiffness When the flexural rigidity of the specimens obtained by static load-displacement test was applied to dynamic vibration analysis, the results were in approximate agreement with experiments. Therefore, relation between the rigidity and the moment of inertia of transformed section in elastic design of R C member was investigated. Yang's modulus of concrete E_c of $295 \times 10^3 \text{ kgf/cm}^2$, $280 \times 10^3 \text{ kgf/cm}^2$ and $270 \times 10^3 \text{ kgf/cm}^2$ were applied for No. 1, No. 2 and No. 3 specimen, assuming $E_c = 40000 f_c^2 (\text{kgf/cm}^2)$. (Ref. 3)

In order to obtain the mean moment of inertia of a column, it is divided into four segments with equal height. At the middle height of each segment, axial compressive force N , bending moment M , depth of neutral axis x and moment of inertia I were calculated, according equations (8) and (9), where n is Yang's modulus ratio of steel to concrete. (Fig. 7)

$$x^3 + 3e'x^2 + 6nA_s(d + d' + 2e')x/b - 6nA_s(d(d + e') + d'(d' + e'))/b = 0 \quad (8)$$

$$I = bx^3/12 + nA_s(d - d')^2/2 + bx(h - x)^2/4 \quad (9)$$

Mean moment of inertia of a column is obtained, assuming that the deflection angle at the top of a column based on it is equal to the sum of deflection angles of four segments. (Table 5)

As measured flexural stiffness is roughly in inverse proportion to displacement, calculated moment of inertia was divided by correction coefficients to express the tendency. These coefficients are $(1.28 + 76\delta/h)$, $(1.03 + 38\delta/h)$ and $(1.22 + 22\delta/h)$ for No. 1, No. 2 and No. 3 specimen respectively, where δ and h are maximum displacement and height of a column. (Table 5)

Calculated flexural stiffness according to design equations was approximately agreed with measured stiffness, as shown in Fig. 10. The reinforcement ratios of No. 1, No. 2 and No. 3 specimen were 2.1 %, 4.3 % and 6.3 % respectively.

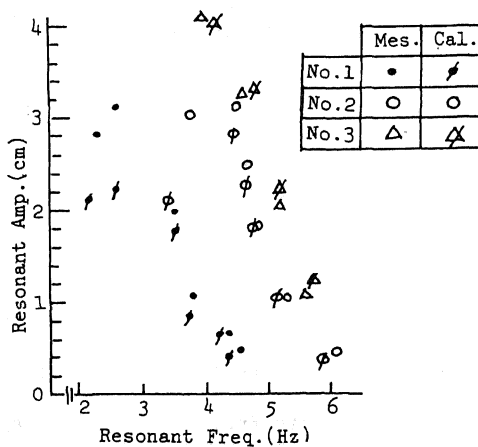


Fig. 9 Resonant Frequency and amplitude Measured and Calculated

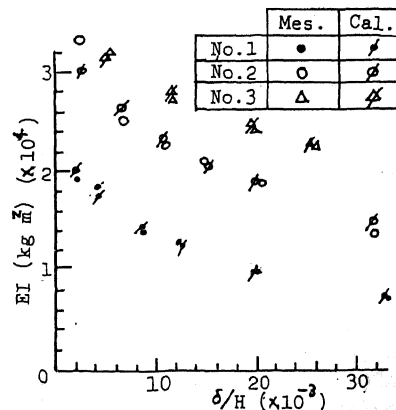


Fig. 10 Flexural Stiffness

Table 5 Moment of Inertia of Transformed Sections of the Column for Load P

No.	P (kg)	x=0.1281 m			x=0.3844 m			x=0.6406 m			x=0.8969 m			I _m
		M/N	x(cm)	I	M/N	x(cm)	I	M/N	x(cm)	I	M/N	x(cm)	I	
1-1	100	29.75	3.529	1003	22.80	2.939	965	15.26	3.091	977	7.05	3.741	1010	986
2	200	59.50	2.766	949	45.59	2.797	953	30.51	2.867	959	14.09	3.131	980	954
3	300	89.25	2.732	946	68.39	2.753	948	45.77	2.797	953	21.13	2.962	967	949
4	400	119.0	2.716	944	91.19	2.731	946	61.03	2.764	949	28.18	2.884	961	947
5	500	148.7	2.706	943	114.0	2.718	945	76.29	2.744	947	35.22	2.838	956	945
6	600	178.5	2.699	943	136.8	2.709	944	91.54	2.739	947	42.27	2.808	954	944
2-1	200	59.50	3.411	1208	45.59	3.445	1210	30.51	3.518	1213	14.09	3.794	1223	1210
2	400	119.0	3.356	1205	91.19	3.373	1206	61.03	3.409	1208	28.18	3.537	1214	1206
3	600	178.5	3.338	1204	136.8	3.348	1205	91.54	3.372	1206	42.27	3.457	1210	1205
4	800	238.0	3.329	1204	182.4	3.337	1204	122.1	3.354	1205	56.36	3.418	1208	1204
5	1000	297.5	3.323	1203	228.0	3.330	1204	152.6	3.344	1204	70.45	3.393	1207	1204
6	1057	314.4	3.323	1203	241.0	3.328	1203	161.3	3.341	1204	74.46	3.389	1207	1204
3-1	400	119.0	3.704	1434	91.19	3.720	1435	61.03	3.757	1436	28.18	3.888	1440	1435
2	800	238.0	3.676	1434	182.4	3.684	1434	122.1	3.702	1434	56.36	3.767	1436	1434
3	1200	357.0	3.667	1433	273.6	3.673	1433	183.1	3.684	1434	84.54	3.727	1435	1433
4	1490	443.3	3.663	1433	339.7	3.668	1433	227.3	3.677	1434	105.0	3.711	1435	1433

M/N = e(cm), M: Bending Moment, N: Axial Load, I: Moment of Inertia (cm⁴), I_m: Mean Moment of Inertia (cm⁴)

The reason why these correction coefficients are large for the member with small reinforcement ratio is thought that the degree of reduction of flexural rigidity due to deformation is comparatively severe to it.

CONCLUSION

It became clear except near failure that statical and dynamical behaviour of R C columns in elastic and plastic domain analysed by linear vibration equations gave fairly good agreement with the experimental results, in which flexural stiffness and damping ratio obtained by the tests were applied. The flexural stiffness for dynamic analysis calculated from the moment of inertia of transformed section in elastic design of R C columns showed in approximate agreement with experiments, modifying by correction coefficients, though cracks occurred in both tension and compression side of columns continuously and inverted S type hysteresis loop appeared in static tests.

The range of tests is very narrow and several things are left unknown to apply practical cases. Also, complicated motion in process of increasing frequency is not clarified yet and more detailed study and experiment are necessary.

ACKNOWLEDGEMENTS

The experiments were performed by students of fourth grade in structure laboratory. The authors wish to express their sincere appreciation to them.

REFERENCES

1. Ray W. Clough and Joseph Penzien, Dynamics of Structures, Mc Graw-Hill Inc. 1975
2. Alan H. Mattock, "Cyclic Shear Transfer and Type of Interface," Proceedings, ASCE, Vol 107, ST 10, October 1981
3. Hajime Okamura and Shoichi Maeda, Reinforced Concrete Engineering, Ichigaya-Syuppan Co.